Charge Transfer Induced Multifunctional Transitions with Sensitive Pressure Manipulation in a Metal−Organic Framework

Junye Yang,[†,‡] Long Zhou,[†,‡] Jinguang Cheng,[†,§] Zhiwei Hu,[∥] Changyang Kuo,[∥] Chih-Wen Pao,[⊥] Lingyun Jang,[⊥] Jyh-Fu Lee,[⊥] Jianhong Dai,[†] Sijia Zhang,[†] Shaomin Feng,[†] Panpan Kong,[†] Zhen Yuan,[†] Jie Yuan,[†] Yoshiya Uwatoko,[§] Tao Liu,*[#] Changqing Jin,[†,‡] and Youwen Long*[†,‡]

[†]Beijing National Laboratory for Condensed Matter Physics, Institute of Physics, Chinese Academy of Sciences, Beijing 100190, China

[‡]Collaborative Innovation Center of Quantum Matter, Beijing 100190, China

[§]Institute for Solid State Physics, University of Tokyo, 5-1-5 Kashiwanoha, Kashiwa, Chiba 277-8581, Japan

[∥]Max-Planck Institute for Chemical Physics of Solids, Nöthnitzer Straße 40, 01187 Dresden, Germany

[⊥]National Synchrotron Radiation Research Center, Hsinchu 30076, Taiwan, R.O.C.

[#]State Key Laboratory of Fine Chemicals, Dalian University of Technology, 2 Linggong Rd., Dalian 116024, China

S Supporting Information

ABSTRACT: The metal−organic framework {[Fe(2,2′-bipyridine)(CN)$_4$]$_2$Co-(4,4′-bipyridine)}·4H$_2$O (Fe$_2$Co-MOF) with single-chain magnetism undergoes an intermetallic charge transfer that converts the Fe$_2$Co charge/spin configurations from Fe$^{3+}_{LS}$−Co$^{2+}_{HS}$−Fe$^{3+}_{LS}$ to Fe$^{2+}_{LS}$−Co$^{3+}_{LS}$−Fe$^{3+}_{LS}$ (LS = low spin, HS = high spin) around 220 K under ambient pressure. A series of coherent phase transitions in structure, magnetism, permittivity and ferroelectricity are found to take place accompanying with the charge transfer, making Fe$_2$Co-MOF a unique ferroelectric single-chain magnet at low temperature. Moreover, our detailed measurements of magnetization, dielectric constant, and Raman scattering under high pressures illustrate that the charge transfer as well as the resulting multifunctional transitions can be readily induced to occur at room temperature by applying a tiny external pressure of about 0.5 kbar. The present study thus provides a pressure well-controllable multifunctional material with potential applications in a broad temperature region across room temperature.
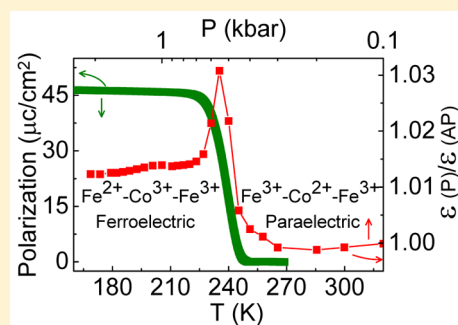
INTRODUCTION

Transition-metal compounds exhibit a wide variety of intriguing physical properties such as superconductivity, colossal magnetoresistance, magnetoelectric coupling multiferroicity, and so on. Intermetallic charge transfer (ICT) can simultaneously change the valence states and electronic configurations of transition-metal ions, and therefore induce dramatic variations in crystal structure, magnetic, and electrical properties.[1−4] For example, giant negative thermal expansion with large volume shrinking, spin disorder−order phase transitions, and metal−insulator transformations were found in a few of charge-transfer perovskite oxides such as BiNiO$_3$, LaCu$_3$Fe$_4$O$_{12}$, and SrCu$_3$Fe$_4$O$_{12}$.[5,6] Moreover, the charge-transfer transitions in these solid-state oxides could be tuned by chemical substitutions and/or external stimuli.

Compared to the rare case of ICT presented in the inorganic solid-state oxide, the ICT was found to occur more often in the metal−organic framework, which possesses a higher flexibility in crystal construction and chemical combination between organic and inorganic components with different functionalities.[7−11] One interesting example comes from the Fe- and Co-included MOF with a chemical formula {[Fe(2,2′-bipyridine)(CN)$_4$]$_2$Co(4,4′-bipyridine)}·4H$_2$O.[12] As shown in Figure 1, the structural framework of Fe$_2$Co-MOF consists of unique Fe and Co centers with the Fe center being coordinated by two N atoms and four cyanide carbon atoms and the Co center located inside a N$_6$ octahedral unit. These centers are bridged together via cyanide units along the c-axis direction, and each Co center is surrounded by four equivalent Fe centers. At ambient conditions, the crystal structure is centrosymmetric with space group $C2/m$. Upon cooling, an Fe−Co ICT takes place around 220 K, giving rise to the changes of valence states of Co and partial Fe ions (Fe$^{3+}_{LS}$−Co$^{2+}_{HS}$−Fe$^{3+}_{LS}$ → Fe$^{2+}_{LS}$−Co$^{3+}_{LS}$−Fe$^{3+}_{LS}$) as well as a high-spin to low-spin variation of Co ions. In sharp contrast to most ICT material systems,[13−17] the ICT in the present Fe$_2$Co-MOF occurs between Co ions and only a portion of Fe ions, dividing the initially equivalent Fe^{3+} ions into two nonequivalent Fe^{2+} and Fe^{3+} ions which may occupy different atomic positions. This nonequivalent charge
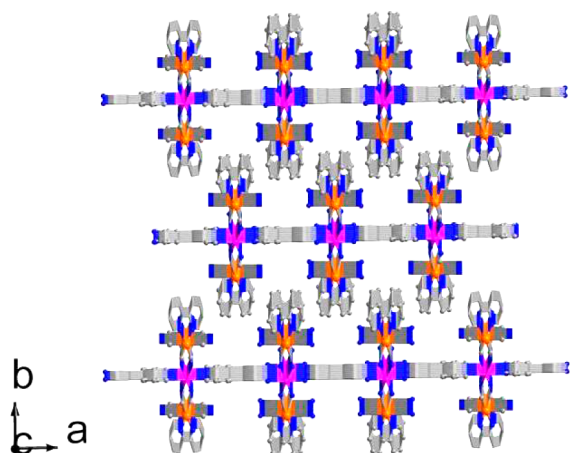
Figure 1. Packing diagram of the two-dimensional layers of Fe_2Co-MOF. H atoms are omitted for clarity. Atomic scheme: Fe, orange; Co, purple; C, gray; N, blue.

redistribution of Fe ions is highly possible to reduce the structure symmetry from the initial nonpolar space group to a polar one and thereby result in a series of functional phase transitions. These coupled transitions in structure, magnetism, permittivity, and ferroelectricity have received much attention in inorganic solid state oxides as promising multifunctional materials such as multiferroics,[18−21] but they are little known in metal−organic frameworks to data.

In this paper, we measured the X-ray absorption spectra (XAS) of Fe_2Co-MOF to confirm that a nonequivalent ICT occurred between Fe and Co ions. As expected from a nonpolar-to-polar structure variation, sharp dielectric and ferroelectric phase transitions are observed accompanying with the Fe−Co ICT. These electric transitions are coupled with a drastic change in magnetization due to the valence and spin state variations of Fe and Co ions. Furthermore, the porous and soft structure of Fe_2Co-MOF provides a unique opportunity to manipulate these multifunctional transitions by external stimuli such as high pressure (HP). Our results show that the present Fe_2Co-MOF displays very sensitive pressure dependence so that a tiny pressure of about 0.5 kbar, which is readily available in industry, is sufficient to move the charge-transfer critical temperature (T_C) to room temperature (RT).

■ EXPERIMENTAL SECTION

High-quality Fe_2Co-MOF samples including powders and single crystals were prepared by a wet chemical method as reported elsewhere.[12] Low-temperature differential scanning calorimetry (DSC) was performed using a Setaram DSC-131 system with temperature scanning in 5 K/min. The valence states of Fe and Co below and above T_C were identified by XAS at the Co-K and Fe-K edges measured at the 16A and 17C beamlines of the National Synchrotron Radiation Research Center in Taiwan, respectively. The temperature dependence of magnetization was measured in a commercial superconducting quantum interference device (MPMS-5, Quantum Design) in zero-field cooling mode under 1 T. The data of dielectric constant (ε) was obtained with an Agilent 4980AL LCR meter on a small single crystal with the size about $250 \times 250 \times 200$ μm^3. The ac frequency we used was 100 kHz. A similar single crystal was adopted to measure the pyroelectric current (I_p) by using an electrometer while sweeping the temperature at a rate of 2 K/min. The electric polarization was then calculated by integrating I_p as a function of time. High-pressure magnetization and dielectric constant were measured through a set of piston−cylinder pressure cells with glycerol as pressure medium, and the pressures were calibrated on the basis of

the pressure dependence of the superconducting transition temperature of Sn metal. High-pressure Raman scattering data were collected at RT on a Renishaw micro-Raman spectroscopy system by using a diamond anvil cell, where the pressures were determined by ruby fluorescence method.[22]

■ RESULTS AND DISCUSSION

To understand the nature of the phase transition caused by the Fe−Co intermetallic charge transfer in Fe_2Co-MOF, DSC measurements were carried out. As shown in Figure 2a, one can
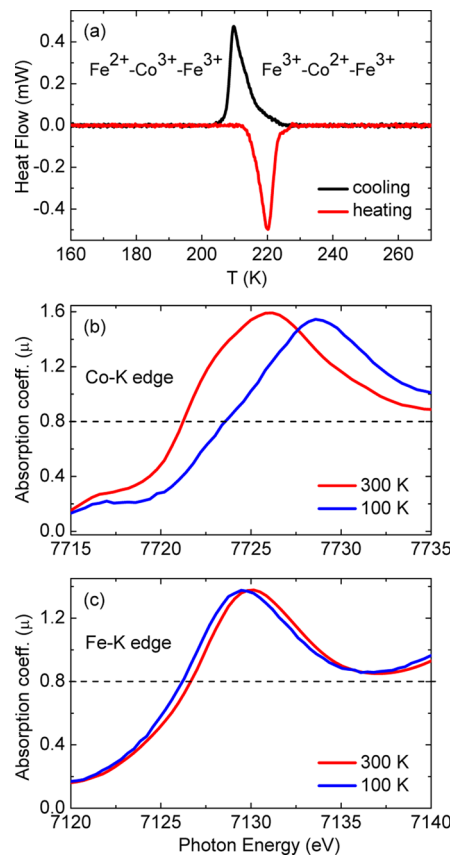

Figure 2. (a) Low-temperature differential scanning calorimetry of Fe_2Co-MOF on cooling and heating, (b) the Co-K XAS, and (c) the Fe-K XAS.

find apparent thermal hysteresis between heating and cooling processes, revealing the first-order nature of this phase transition. The T_C determined by the endothermic peak on heating is about 220 K, whereas it decreases to about 210 K on cooling. In this paper, we use the heating T_C to present all the coherent phase transitions caused by the Fe−Co ICT.

It is well-known that the X-ray absorption spectrum at the transition metal K edge is very sensitive to the valence state of transition metal.[23,24] This technique is used to identify the valence states of Fe and Co ions in the present Fe_2Co-MOF. Figure 2b shows the Co-K XAS measured at 300 and l00 K. As judged from the absorption edge (defined at $\mu = 0.8$)[24] around 7721.2 eV at 300 K, it undergoes a significant shift toward a higher energy by about 2.5 eV with decreasing temperature to 100 K, providing convincing evidence for the valence state change of Co ions from +2 (above T_C) to +3 (below T_C). By comparison, the spectrum at the Fe-K edge shifts toward a lower energy on cooling. Moreover, the magnitude of energy shift determined from the absorption edge at $\mu = 0.8$ is not so

remarkable between 300 and 100 K (~0.5 eV, see Figure 2c). These observations suggest that only a portion of Fe^{3+} ions are converted to Fe^{2+} during the charge transfer. The present XAS results therefore confirm the proposed charge-transfer transition from the high-temperature $Fe^{3+}-Co^{2+}-Fe^{3+}$ charge phase with uniform Fe^{3+} states to the low-temperature $Fe^{2+}-Co^{3+}-Fe^{3+}$ one with distinct Fe^{2+} and Fe^{3+} states.[12] Note that, due to the 1D-chain structure, the Fe–Co ICT most probably occurs within the chains along the c-axis.

Since the electronic configurations of Fe and Co ions are changed essentially by the charge transfer, it is expected to see joint functional transitions in the present Fe_2Co-MOF. As illustrated by the temperature dependence of magnetization and its derivative in Figure 3a, with decreasing temperature
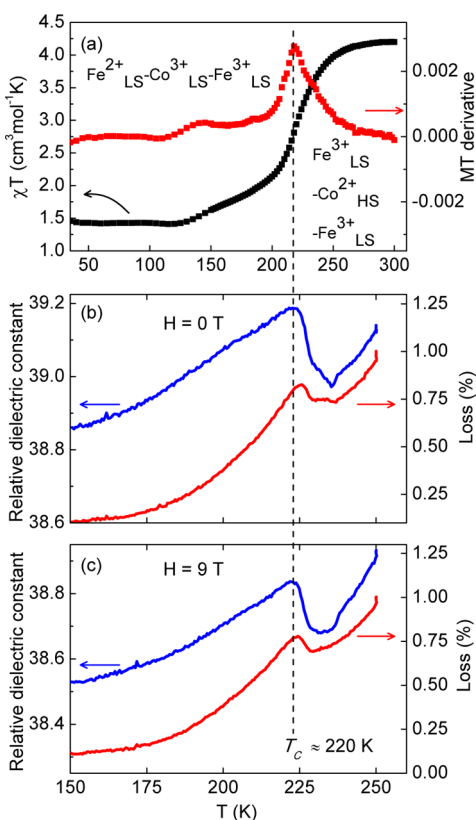

Figure 3. Temperature dependence of (a) magnetization and its derivative, and relative dielectric constant and the dielectric loss measured at (b) zero field and (c) 9 T.

close to the T_C, the magnetization undergoes a drastic decrease, which is attributed to a paramagnetism-to-diamagnetism transition due to the CT-induced high-spin Co^{2+} (S = 3/2) to low-spin Co^{3+} (S = 0) variation as well as partial Fe^{3+}_{LS} (S = 1/2) to Fe^{2+}_{LS} (S = 0) transition ($Fe^{3+}_{LS}-Co^{2+}_{HS}-Fe^{3+}_{LS} \rightarrow Fe^{2+}_{LS}-Co^{3+}_{LS}-Fe^{3+}_{LS}$).[12] Moreover, this magnetic change is closely coupled with permittivity variation. As shown in Figure 3b, the dielectric constant as well as the dielectric loss also experiences a remarkable anomaly around the T_C. When a magnetic field is applied to measure the dielectric constant, we do not find significant field response on permittivity near the T_C. As presented in Figures 3b and 3c, the dielectric peak is almost unchanged at zero field and 9 T.

The presence of dielectric peak is indicative of ferroelectric polarization. The ferroelectricity is further confirmed by pyroelectric current measurements. The poling electric field E

= 600 kV/m is applied from 270 K down to 2 K, and then the electric field is turned off and the sample is shorted for half an hour before warming up. As shown in Figure 4a, a sharp
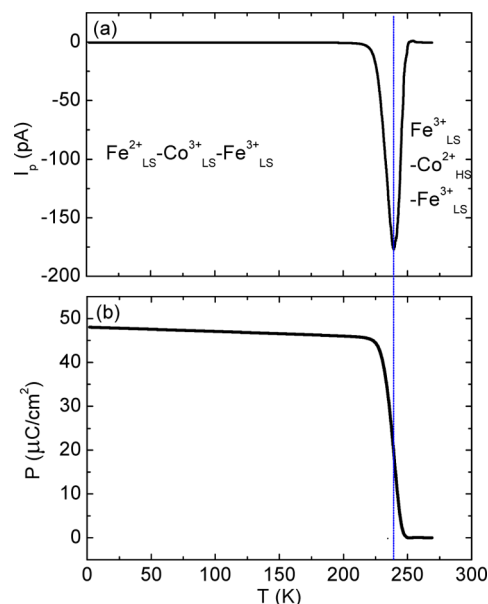

Figure 4. Temperature dependence of (a) pyroelectric current I_p and (b) polarization of Fe_2Co-MOF measured at ambient pressure.

pyroelectric dip appears near the T_C, strongly suggesting the presence of electric polarization accompanying with the charge transfer. When we integrate the I_p as a function of time, the temperature dependent polarization is obtained as shown in Figure 4b. The striking increase of polarization around the T_C confirms a paraelectricity-to-ferroelectricity transition due to the variation of charge combination from the high-temperature $Fe^{3+}-Co^{2+}-Fe^{3+}$ with uniform Fe^{3+} ions to the low-temperature $Fe^{2+}-Co^{3+}-Fe^{3+}$ with nonequivalent Fe^{2+} and Fe^{3+} states. The observation of ferroelectric hysteresis loops below the T_C further reveals the occurrence of ferroelectric phase transition (see Supporting Information). These results clearly show that the unusual Fe–Co ICT does lead to a series of coherent magnetoelectric phase transitions and the present Fe_2Co-MOF can be regarded as a promising multifunctional material.[25] Moreover, Fe_2Co-MOF shows single-chain magnetic behavior with intrachain ferromagnetic interactions at low temperature (<10 K).[12] The CT-induced electric polarization indicates the coexistence of magnetic and ferroelectric degrees of freedom,[26] making Fe_2Co-MOF a unique ferroelectric single-chain magnet.

As is well-known, MOF usually possesses a porous and soft structure, so it is expected that external high pressure can play a critical role on the structure and physical properties. We therefore applied HP to manipulate the Fe–Co intermetallic charge transfer of the present Fe_2Co-MOF. Figure 5 shows the temperature dependence of magnetization measured at different pressures. Obviously, when the sample is subjected to a minute pressure, the T_C determined by magnetization derivative shifts quickly to higher temperatures, and reaches 280 K at 0.30 kbar (Figure 6a). Above this pressure, it is difficult to precisely determine the T_C due to the limited temperature range (2–300 K) in this experiment, but we can see that the T_C approaches RT around 0.50 kbar. Note that when the pressure is released from the maximum value of 2.05
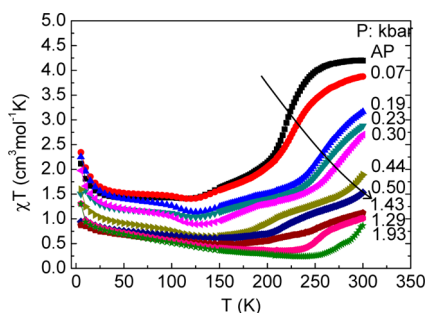
Figure 5. Temperature dependence of magnetization of Fe_2Co-MOF measured at different pressures. The solid line with arrow is guide for eyes for the shift of charge transfer.

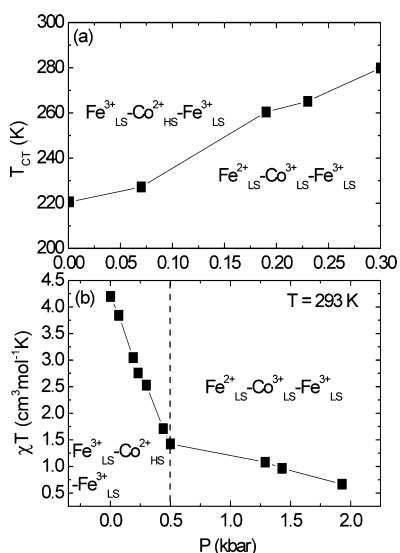**Figure 6.** Pressure dependence of (a) charge-transfer temperature and (b) the value of magnetization of Fe_2Co-MOF obtained at 293 K. The solid line in plot (a) shows the linear fitting.

kbar used here to ambient pressure (AP), the T_C is completely reversible (not shown in Figure 5).

Figure 6a presents the pressure dependence of T_C in the pressure range between AP and 0.30 kbar. A linear fitting to $T_C(P)$ yields a value of $dT_C/dP \approx 207$ K/kbar. In comparison with other organic and inorganic compounds exhibiting ICT, such a pressure dependence of T_C is unusually huge. For example, the Fe−Co ICT in a Prussian blue analogue $K_{0.1}Co_4[Fe(CN)_2]_{2.7}\cdot18H_2O$ was found to increase with pressure at a rate of only 17 K/kbar, which was smaller than the present one by 1 order of magnitude.[27] Recently, a pressure−temperature phase diagram was reported for the ferroelectric phase transition in a supramolecular crystal of anilic acids and 2,3-di(2-pyridinyl)pyrazine, and a similar change rate (19 K/kbar in average) with that of the Prussian blue analogue was observed.[28] As for the ICT observed in the inorganic oxide materials, the pressure dependence of T_C becomes even smaller. For instance, the values of dT_C/dP were determined to be ∼13 K/kbar and only 3 K/kbar for $BiNiO_3$ and $LaCu_3Fe_4O_{12}$, respectively.[6,29] The supersensitive pressure dependence of the Fe−Co ICT observed in the present Fe_2Co-MOF should be related to its special crystal structure. As shown in Figure 1, Fe_2Co-MOF crystallizes in an incompact layered structure, where there exist a large number of structural voids between the layers. As a consequence,

external pressure can readily compress the unit cell volume and trigger the Fe−Co ICT at elevated temperatures. These results confirm that the application of external pressure is a highly effective method to tune the ICT as well as the coherent physical properties in the present Fe_2Co-MOF.

To determine the room-temperature critical pressure (P_C) of the charge transfer in Fe_2Co-MOF, we plotted the magnetization values obtained at 293 K as a function of pressure in Figure 6b. Obviously, the magnetization first decreases significantly with increasing pressure up to about 0.5 kbar, and then decreases slightly at higher pressures. Based on this observation, the pressure ∼0.5 kbar is tentatively assigned as the room-temperature P_C, which is a quite small and readily available pressure value in industry. By comparison, the Fe−Co ICT of $K_{0.1}Co_4[Fe(CN)_2]_{2.7}\cdot18H_2O$ cannot occur until the pressure exceeds 4.0 kbar at RT,[27] and 20−30 kbar pressure is required to induce the Cu−Fe ICT in $LaCu_3Fe_4O_{12}$.[29]

The above observations indicate that the application of HP can readily stabilize the ferroelectric state of the charge-transferred Fe_2Co-MOF at RT. To further elaborate this deduction, we measured the high-pressure permittivity at room temperature. As shown in Figure 7a, the normalized dielectric
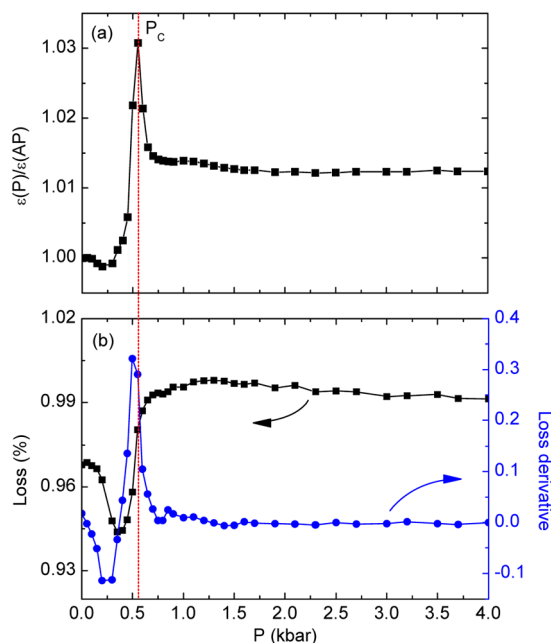

Figure 7. Pressure dependence of (a) normalized dielectric constant and (b) dielectric loss and its derivative of Fe_2Co-MOF measured at room temperature.

constant ($\varepsilon_n = \varepsilon(P)/\varepsilon(AP)$) gradually decreases with increasing pressure to 0.2 kbar owing to the size effect under compression, and then the ε_n starts to sharply increase and rises to a maximum value around 0.55 kbar, which is consistent with the P_C estimated from the magnetization data (Figure 6b). Above 1.0 kbar, the ε_n is almost constant with pressure. These characteristic features are reminiscent of a pressure-induced ferroelectric phase transition as observed in other compounds.[30,31] As shown in Figure 7b, near the P_C, the derivative of dielectric loss also shows a sharp transition. We therefore conclude that the room-temperature ferroelectric phase is indeed realized in Fe_2Co-MOF via the application of external pressure accompanying the Fe−Co ICT. On account of the pressure supersensitivity of the charge transfer as well as a series

of coherent magnetoelectric transitions, the present Fe_2Co-MOF provides a promising candidate for pressure well-controllable multifunctional materials in a wide temperature region across the RT.

As mentioned before, different from most charge-transfer compounds, the ICT of Fe_2Co-MOF takes place between Co and partial Fe ions, converting the equivalent Fe^{3+} states to nonequivalent Fe^{2+} and Fe^{3+} states. This unusual behavior is presumably caused by the different bonding types of Fe centers via hydrogen bonds between uncoordinated water molecules and terminal cyanide nitrogen atoms. Note that similar charge-transfer behavior was also found in an analogous Fe_2Co-included MOF.[32] The distinct coordination environments of Fe ions may reduce the structural symmetry of the initial $C2/m$ space group, leading to a nonpolar-to-polar phase transition. Therefore, it is very interesting to clarify the crystal structure of the charge-transferred $Fe^{2+}-Co^{3+}-Fe^{3+}$ phase. Unfortunately, the reported low-temperature X-ray diffraction cannot resolve the crystal structure probably due to the similar diffraction between the initial $Fe^{3+}-Co^{2+}-Fe^{3+}$ phase and the charge-transferred $Fe^{2+}-Co^{3+}-Fe^{3+}$ phase as well as the fact that X-ray is not sensitive to light elements such as H, C, O, and N involved in the present Fe_2Co-MOF system.[12] We then resorted to high-pressure Raman scattering at RT to study the CT-induced structural transition.

Figure 8 presents some typical high-pressure Raman scattering patterns measured at RT. Two characteristic features
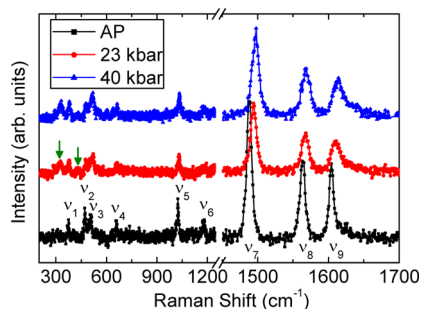

Figure 8. High-pressure Raman scattering patterns of Fe_2Co-MOF measured at room temperature.

are observed. First, the nine visible Raman peaks (ν_1, ν_2, ..., ν_9) identified at AP systematically shift toward higher frequencies with elevating pressure due to the contraction of interatomic distances. Second, above the P_C, two new Raman vibration modes marked with arrows are found clearly around 320 and 425 cm^{-1}, respectively, providing convincing evidence for structural phase transition. Since all the ambient-pressure Raman vibrations remain robust well above the P_C, the high-pressure phase most probably adopts a subgroup of the initial $C2/m$ space group, i.e., either $C2$ or Cm. According to the symmetry analysis, both $C2$ and Cm space groups are noncentrosymmetric and belong to the polar point groups (2 and m, respectively), which allow the occurrence of ferroelectric polarization as we observed in experiments. For a full resolution of the polar $Fe^{2+}-Co^{3+}-Fe^{3+}$ structure, neutron diffraction should be desirable in the future.

CONCLUSIONS

In conclusion, the Fe—Co intermetallic charge transfer from the high-temperature $Fe^{3+}_{LS}-Co^{2+}_{HS}-Fe^{3+}_{LS}$ phase to the low-temperature $Fe^{2+}_{LS}-Co^{3+}_{LS}-Fe^{3+}_{LS}$ phase is confirmed by the

XAS method in Fe_2Co-MOF. This charge transfer occurring at about 220 K leads to a series of coherent phase transitions in structure, magnetism, dielectricity, and ferroelectricity. Since this compound shows single-chain magnetism with intrachain ferromagnetic interactions at lower temperatures, magnetic and ferroelectric degrees of freedom coexist, making Fe_2Co-MOF a unique ferroelectric single-chain magnet. In addition, we also studied pressure effects on the ICT by high-pressure magnetization, dielectric constant, and Raman scattering measurements. Due to the incompact 1D-chain structure, this material exhibits supersensitive pressure response. A huge pressure change rate of T_C (207 K/kbar) and a quite small room-temperature critical pressure (~0.5 kbar) are found. In sharp contrast to most charge-transfer compounds where all the transition-metal ions take part in the charge redistribution, the ICT in the present Fe_2Co-MOF occurs between Co ions and only a portion of Fe ions, dividing the equivalent Fe^{3+} ions into two nonequivalent Fe^{2+} and Fe^{3+} ions. As a consequence, the crystal symmetry is reduced as confirmed by high-pressure Raman scattering. On the basis of structural symmetry analysis, a polar space group ($C2$ or Cm) with ferroelectricity is tentatively assigned to the charge-transferred $Fe^{2+}-Co^{3+}-Fe^{3+}$ phase. On account of the ICT-induced multiple physical property changes, the present Fe_2Co-MOF opens up a new direction for searching pressure well-controlled multifunctional materials with a wide working temperature window.

ASSOCIATED CONTENT

Ⓢ Supporting Information

Listing of ferroelectric hysteresis loop of Fe_2Co-MOF measured at 10 K. The Supporting Information is available free of charge on the ACS Publications website at DOI: 10.1021/acs.inorgchem.5b00739.

AUTHOR INFORMATION

Corresponding Authors

*E-mail: liutao@dlut.edu.cn.

*E-mail: ywlong@iphy.ac.cn.

Notes

The authors declare no competing financial interest.

REFERENCES

(1) Horiuchi, S.; Okimoto, Y.; Kumai, R.; Tokura, Y. *Science* **2003**, *299*, 229–232.

(2) Alves, H.; Molinari, A. S.; Xie, H.; Morpurgo, A. F. *Nat. Mater.* **2008**, *7*, 574–580.

(3) Long, Y. W.; Hayashi, N.; Saito, T.; Azuma, M.; Muranaka, S.; Shimakawa, Y. *Nature* **2009**, *458*, 60–64.

(4) Huang, Z.; Auckett, J. E.; Blanchard, P. E. R.; Kennedy, B. J.; Miiller, W.; Zhou, Q.; Avdeev, M.; Johnson, M. R.; Zbiri, M.; Garbarino, G.; Marshall, W. G.; Gu, Q.; Ling, C. D. *Angew. Chem. Int. Ed.* **2014**, *53*, 3414–3417.

(5) Yamada, I.; Tsuchida, K.; Ohgushi, K.; Hayashi, N.; Kim, J.; Tsuji, N.; Takahashi, R.; Matsushita, M.; Nishiyama, N.; Inoue, T.; Irifune,

T.; Kato, K.; Takata, M.; Takano, M. *Angew. Chem. Int. Ed.* **2011**, *50*, 6579−6582.

(6) Azuma, M.; Chen, W.; Seki, Hayato.; Czapski, M.; Olga, S.; Oka, K.; Mizumaki, M.; Watanuki, T.; Ishimatsu, N.; Kawamura, N.; Ishiwata, S.; Tucker, M. G.; Shimakawa, Y.; Attfield, J. P. *Nat. Commun.* **2011**, *2*, 347.

(7) Kreno, L. E.; Leong, K.; Farha, O. K.; Allendorf, M.; Van Duyne, R. P.; Hupp, J. T. *Chem. Rev.* **2012**, *112*, 1105−1125.

(8) Tan, J. C.; Cheetham, A. K. *Chem. Soc. Rev.* **2011**, *40*, 1059−1080.

(9) O'Keeffe, M.; Yaghi, O. M. *Chem. Rev.* **2012**, *112*, 675−702.

(10) Wang, C.; Zhang, T.; Lin, W. *Chem. Rev.* **2012**, *112*, 1084−1104.

(11) Zhang, W.; Xiong, R. G. *Chem. Rev.* **2012**, *112*, 1163−1195.

(12) Liu, T.; Zhang, Y. J.; Kanegawa, S.; Sato, O. *J. Am. Chem. Soc.* **2010**, *132*, 8250−8251.

(13) Long, Y. W.; Shimakawa, Y. *New J. Phys.* **2010**, *12*, 063029.

(14) Podgajny, R.; Chorazy, S.; Nitek, W.; Rams, M.; Majcher, A. M.; Marszałek, B.; Zukrowski, J.; Kapusta, C.; Sieklucka, B. *Angew. Chem. Int. Ed.* **2013**, *52*, 896−900.

(15) Cafun, J. D.; Lejeune, J.; Baudelet, F.; Dumas, P.; Itié, J. P.; Bleuzen, A. *Angew. Chem. Int. Ed.* **2012**, *51*, 9146−9148.

(16) Higel, P.; Villain, F.; Verdaguer, M.; Rivière, E.; Bleuzen, A. *J. Am. Chem. Soc.* **2014**, *136*, 6231−6234.

(17) Long, Y. W.; Saito, T.; Tohyama, T.; Oka, K.; Azuma, M.; Shimakawa, Y. *Inorg. Chem.* **2009**, *48*, 8489−8492.

(18) Kimura, T.; Goto, T.; Shintani, H.; Ishizaka, K.; Arima, T.; Tokura, Y. *Nature* **2003**, *426*, 55−58.

(19) Spaldin, N. A.; Fiebig, M. *Science* **2005**, *309*, 391−392.

(20) Eerenstein, W.; Mathur, N. D.; Scott, J. F. *Nature* **2006**, *442*, 759−765.

(21) Cheong, S.-W.; Mostovoy, M. *Nat. Mater.* **2007**, *6*, 13−20.

(22) Mao, H. K.; Xu, J.; Bell, P. M. *J. Geophys. Res.* **1986**, *91*, 4673−4676.

(23) Croft, M.; Sills, D.; Greenblatt, M.; Lee, C.; Cheong, S.-W.; Ramanujachary, K. V.; Tran, D. *Phys. Rev. B* **1997**, *55*, 8726−8732.

(24) Poltavets, V. V.; Croft, M.; Greenblatt, M. *Phys. Rev. B* **2006**, *74*, 125103.

(25) Hoshino, N.; Iijima, F.; Newton, G. N.; Yoshida, N.; Shiga, T.; Nojiri, H.; Nakao, A.; Kumai, R.; Murakami, Y.; Oshio, H. *Nat. Chem.* **2012**, *4*, 921−926.

(26) Ohkoshi, S.; Tokoro, H.; Matsuda, T.; Takahashi, H.; Irie, H.; Hashimoto, K. *Angew. Chem. Int. Ed.* **2007**, *46*, 3238−3241.

(27) Ksenofontov, V.; Levchenko, G.; Reiman, S.; Gütlich, P.; Bleuzen, A.; Escax, V.; Verdaguer, M. *Phys. Rev. B* **2003**, *68*, 024415.

(28) Horiuchi, S.; Kumai, R.; Tokura, Y. *J. Am. Chem. Soc.* **2013**, *135*, 4492−4500.

(29) Long, Y. W.; Kawakami, T.; Chen, W.; Saito, T.; Watanuki, T.; Nakakura, Y.; Liu, Q. Q.; Jin, C. Q.; Shimakawa, Y. *Chem. Mater.* **2012**, *24*, 2235−2239.

(30) Fujimoto, S.; Yasuda, N.; Kashiki, H. *J. Phys. D: Appl. Phys.* **1982**, *15*, 487−495.

(31) Hikita, T.; Maruyama, T. *J. Phys. Soc. Jpn.* **1992**, *61*, 2840−2847.

(32) Dong, D. P.; Liu, T.; Kanegawa, S.; Kang, S.; Sato, O.; He, C.; Duan, C. Y. *Angew. Chem. Int. Ed.* **2012**, *51*, 5119−5123.